Research Article

Journal of Environmental Nanotechnology

A Review on Carbonation of Concrete and its Predictive Modelling

Kunal Tongaria[1*], S. Mandal[2], Devendra Mohan[2]

[1]Department of Civil Engineering, Indian Institute of Technology (BHU), Varanasi, UP, India

[2]Professor, Department of Civil Engineering, Indian Institute of Technology (BHU), Varanasi, UP, India

Received: 10.09.2018 Accepted: 14.11.2018 Published: 30-12-2018

*kunal.tongaria.civ13@iitbhu.ac.in

ABSTRACT

The phenomenon of concrete carbonation is a well-researched field. With the ever-rising concern about pollution in the environment, the need for understanding this phenomenon has increased manyfold. Although plenty of experimental data is available, useful and quantifiable generalization of influences of different factors affecting various parameters is a difficult task owing to the innumerable variability in experimental conditions and ingredients of the concretes tested and the specimens taken. Several studies have employed numerical and statistical modelling techniques to predict the depth of carbonation as a function of the age of concrete, compressive strength and other parameters affecting the carbonation of concrete. This paper was aimed at discussing several issues of uncertainty in the prediction and evaluation of carbonation propagation.

Keywords: Carbonation; micro-structure of concrete; Service life; Durability.

1. INTRODUCTION

The physical, mechanical and chemical properties of both components of Reinforced concrete structures (steel and concrete) improve by their synergy. The steel is protected by a concrete layer from various physical and chemical agents, which solves the major problem that affects metallic structures, namely the corrosion of steel when exposed to the environment. (Parrott, 1987; Kulakowski *et al.* 2009).

Corrosion of reinforcement is repressed to some extent due to the high pH of concrete, which is around 12 to 13. A protective oxide layer is formed on the surface of steel which impedes metals from dissolving. However, this protective layer is destroyed when the alkalinity of encompassing concrete gets reduced (Parrott, 1987; Broomfield, 2006; Khan and Lynsdale 2002). Ingress of aggressive nano-level materials like carbon dioxide and chloride ions takes place through the random porous structure of concrete. Due to the carbonation reaction taking place between carbon dioxide and hydration products of cement, carbonates are formed, which causes the reduction in alkalinity of concrete. The reduction in alkalinity also reduces concrete's ability to protect the steel reinforcement from corrosion (Verbeck, 1975; Parrott, 1992; Ho and Lewis 1987; Wierig, 1984). Hobbs (Hobbs 1988) suggested that the threshold value of pH for steel de-passivation is 9.5, below which the steel corrosion takes place, since carbonates formed occupies a greater volume than hydroxides which it replaces and the porosity of carbonated concrete is reduced. Moreover, water released by hydroxides on carbonation may aid the hydration of un-hydrated cement. These changes result in increased surface hardness, increased strength at the surface (Baba and Senbu 1987), reduced surface permeability, reduced moisture movement (Papadakis *et al.* 1991) and increased resistance to those forms of deteriorating attacks that are controlled by porosity (Burkan Isgor and Razaqpur, 2004). It is well known that carbonation also causes an increase in all mechanical properties of concrete like strength, modulus of elasticity and shrinkage of the concrete (Chang *et al.* 2003).

1.1. Mechanism of Carbonation

The process of carbonation of concrete is a combination of various physical and chemical processes. The carbon dioxide is present in the ambient atmosphere or internal air in the buildings. The instrumental mechanism of carbonation is the reaction of diffused CO_2 with calcium hydroxide. The final products of this reaction are $CaCO_3$ and water. The physico-chemical processes involved in carbonation are (Thiery *et al.* 2007):

(1) The diffusion of CO_2 in the gaseous phase of the concrete pores.

(2) The dissolution of CO_2 in the pore water as carbonic acid.

(3) Dissociation of CO_2 as H_2CO_3 and CO_3^{2-} ions.

(4) The dissolution of solid $Ca(OH)_2$.

(5) Releasing of calcium: Ca^{2+} and hydroxyl OH^- ions.

(6) And the precipitation of Ca^{2+} with CO_3^2, forming $CaCO_3$

These intermediate reactions are represented in the following overall chemical reaction given in Eqn. (1):

$$Ca(OH)_2 + CO_2 \rightarrow CaCO_3 + H_2O \quad (1)$$

Apart from $Ca(OH)_2$, several other hydration compounds also react with CO_2. The reaction between CO_2 and the calcium silicate hydrates ($C-S-H$) produces $CaCO_3$ and a silica gel (Šauman, 1971; Slegers and Rouxhet 1976; Kobayashi *et al.* 1994). In the case of a rapid-hardening cement with a high C_3A content or cement mixed with a large amount of gypsum, Ettringite (tri-sulfate hydrates AFt) and mono-sulfate hydrates (AFm) are also formed in abundance (Thiery *et al.* 2007).

1.2 Carbonation: a Non-linear Phenomena

Many studies have been carried out on the carbonation of concrete. However, the generalization of observed trends seems to be an almost impossible task as there are innumerable variations in experimental conditions and compositions of the concretes tested.

The above-mentioned processes (Section 1.1) are governed by their own factors, which are interdependent. For example, the diffusion of CO_2 is dependent upon the transport properties of the concrete structure. These transport properties are governed by moisture content, type of cement and temperature of the media. As seen in the chemical reaction, water is formed at the end of the reaction. This will affect the diffusion of CO_2 and water (Lagerblad, 2005). Because of these coupling or synergic effects of influencing parameters involved at almost every step of the process, any analytical model for the prediction of carbonation is inherently complex and should be based on a non-linear scheme.

For reinforced concrete structures, the onset of reinforcement corrosion is considered as one of the critical stages for determining the service life of a concrete structure (Khunthongkeaw *et al.* 2006). Carbonation is a process from the surface, i.e., the amount of carbonated nano-material is related to exposure time and surface. Surfaces in direct contact with carbon dioxide and water will carbonate rapidly, but a shell of already carbonated concrete will slow down the carbonation of the interior. The rate of carbonation is not constant. The carbonation will eventually slow down as the carbon dioxide must pass through a thickening layer of concrete's altered products (Lagerblad, 2005).

2. OVERVIEW OF SOME CARBONATION MODELS PROPOSED

Based on many experimental studies in the past, along with analytical hypotheses proposed by many authors, several mathematical models have been developed to predict the concrete service life of the structure.

Several early experimental studies on concrete carbonation for outdoor conditions (Shigeyoshi Nagataki and Eun Kyum Kim 1986) and for controlled indoor conditions (Tuutti 1982; Shigeyoshi Nagataki and Eun Kyum Kim 1986; S. Nagataki and H. Ohga 1988; Qiu-Dong 1987) hypothese that depth of concrete carbonation or the location of "carbonation front" is directly proportional to the square root of the age of concrete. i.e., $\sqrt{t}$ (Papadakis Vayenas *et al.* 1991). The expression used is applied in Eqn. (2),

$$X_c = A\sqrt{t} \quad (2)$$

where, X_c = carbonation depth after time t, t = carbonation exposure duration, and A = empirical constant.In this model, it is to be noted that the variable nature of the diffusivity constant of CO_2 was not considered (Houst and Wittmann 2002). In reality, the value of A should depend upon the degree of saturation of concrete, the pore structure of concrete and the carbon dioxide content of the environment.

A more accurate model based on the microstructure of concrete, which is quite similar to Eqn. 2 was developed by (Papadakis Vayenas *et al.* 1991). This mathematical model yielded a complex non-linear system of differential equations in space and time and had to be solved numerically for the unknown concentrations of the materials involved (Papadakis Fardis *et al.* 1991). This model predicted Eqn. (3), for giving depth of carbonation:

$$X_c = \sqrt{\frac{2D^C_{e,CO_2}[CO_2]^0}{[Ca(OH)_2]^0 + 3[CSH]^0 + 3[C_3S]^0 + 2[C_2S]^0}t} \quad (3)$$

where, D^C_{e,CO_2} = effective diffusivity of CO_2 and $[Ca(OH)_2]^0$, $[Ca(OH)_2(s)]^0$, $[CSH]^0$, $[C_3S]^0$ and $[C_2S]^0$ are the "initial" concentrations (at t=0) of $Ca(OH)_2(aq)$, $Ca(OH)_2(s)$, CSH, C_3S, and C_2S respectively at the end of moist curing. In this model, carbonation effects of anhydrous cement clinker phases, concrete porosity and degree of saturation were also taken into account. The proposed model could predict the test results of previous researchers for exposure to natural or higher concentrations of ambient CO_2.

There are other several statistical and linear regression-based models available for the relationship among influencing factors, carbonation depth and strength (Taffese *et al.* 2015; Atiş 2004; Leemann *et al.* 2015; Hills *et al.* 2015; J.-K. Kim and Lee, 1999).

Apart from empirical models, several finite element-based models (Burkan Isgor and Razaqpur 2004; H.-W. Song *et al.* 2006; Hussain 2011) have been used to predict the temporal variation of carbonation depth. A non-linear finite element approach for tracing the spatial and temporal advancement of the carbonation front in concrete structures with and without cracks was developed by (Burkan Isgor and Razaqpur, 2004). A two-dimensional Windows-based finite element computer program, called CONDUR, was developed. The diffusion of carbon dioxide into concrete was modelled as an analogy with a two-dimensional transient heat transfer problem. The dependency of carbon dioxide diffusion rate on the moisture and the temperature was considered. Similarly, moisture transport was also simulated. The progress of carbonation reaction at each time step was determined using chemical kinetics data available. A coupling mechanism between all these processes was achieved using source/sink terms in each process. The relative humidity or the moisture present and concentration of CO_2 in each element were updated at each time step. To determine the onset of rebar corrosion, the time-dependent reduction in pH due to carbonation was determined by using data related to the progress of the carbonation reaction (Eqn. 4). The results obtained from the program were compared with available experimental data.

More recently, a Finite elemental framework developed by Behrouz Shafei (Shafei *et al.* 2012), evaluated the effects of the most critical parameters that may accelerate or slow down the carbonation process. The analyses of parameters are also based on the analogy of several processes involved in concrete carbonation with transient thermal analysis with appropriate modifications. The novelty of the proposed framework was to consider the non-linear time-dependent characteristics of the involved parameters along with their mutual interactions in ANSYS software.

Artificial neural networks and other machine learning techniques have also been used (Liu *et al.* 2008; Kwon and Song 2010; Taffese *et al.* 2015), as it is very difficult to establish a universal carbonation model which can represent all factors because of the numerous influencing factors of carbonation and large data discretization in the laboratory testing or actual site. Artificial neural networks can be very efficiently utilized for this purpose (Liu *et al.* 2008).

A Radial Basis Function (RBF) neural network-based model has been established by Liu *et al.* 2008. Water-gel ratio, cement content and time of exposure of concrete were selected as input parameters in the study, while the output layer had only one node, i.e., carbonation depth of concrete. 72 groups of carbonation data were used in building RBF and BP neural network models, among which 60 groups of data were used to train and another 12 groups of data were used for validation of the model. The prediction results show that the forecast results conform to the test results very well. Through the comparison of results, it was concluded that the RBF neural network is more superior to BP network in both identifying effect and evaluation precision.

Apart from actual carbonation depth, ANNs can be very useful in the determination of several other parameters like diffusion coefficient. In the study (Kwon and Song 2010), different experimental results were analyzed to obtain the comparable data set of the CO_2 diffusion coefficient. Several mix design components (i.e., cement content, water to cement ratio and volume of aggregate including exposure condition of relative humidity) were selected as neurons, followed by training of learning for a neural network using the back-propagation algorithm. The diffusion coefficients of CO_2 obtained from the neural network were found to be in good agreement with experimental data considering various conditions. Finally, the numerical technique, which is based on behavior in early- aged concrete such as hydration and pore structure, was developed considering CO_2 diffusion coefficient from the neural network and changing effect on porosity under carbonation.

3. DISCUSSION: EXPERIMENTAL STUDIES AND PREDICTION MODELS FOR DIFFERENT INFLUENCING FACTORS

A need to review the already existing findings and facts is evolved to help in paving the way for further investigations. So, the effects of the several factors affecting carbonation and environmental loading, which affect the service life of concrete structures, are described in detail. The models proposed and issues of uncertainty in the prediction and evaluation of carbonation propagation are also discussed in this section.

3.1 Effect of Curing Condition

The influence of curing on concrete carbonation can be in terms of the type of curing and in terms of the initial curing period. Conclusions drawn upon the impact of curing may also be different for natural long-term carbonation with site-curing and accelerated carbonation with laboratory-controlled curing. In a critical review by Ekolu, 2016, the author points out that the studies on the effects of different curing methods on natural carbonation of concrete in real structures are very rare. Different methods of curing have been studied in the laboratory, including heat curing (Neville, 1995; Ekolu,

2006; Lo *et al.* 2016), air curing, moisturizing (Neville, 1995; Lo and Lee, 2002; Aprianti *et al.* 2016; Balayssac *et al.* 1995) and use of curing compounds (Neville, 1995; Xue *et al.* 2015).

In an experimental study, (Lo and Lee, 2002) prepared three different normal weight concrete grades A, B and C with water-cement ratios of 0.38, 0.46 and 0.54, respectively, to study the effects of the initial curing method on the depth of carbonation. The details of 3 mixes are given in Table 1.

Table 1. Mix proportion per cubic meter of concrete

Properties	Mix A	Mix C	Mix C
w/c Ratio	0.38	0.46	0.54
OPC (kg)	450	450	450
20 mm granite aggregate (kg)	665	655	645
10 mm granite aggregate (kg)	530	515	510
Rock fines (kg)	535	525	515
Superplasticizer (ml)	2400	0	0

For each grade, 8 cubes of 100 mm size and 8 units of Ø 100 × 200 mm (height) cylinders were cast and stored in water at 27 ± 3 °C. After 28 days, the cubes were tested for compressive strength. The cylinders were taken out from the carbonation chamber after 30, 60 and 90 days and were split in a tensile splitting test. The transverse exposed surfaces were cleaned and tested for carbonation depth using a phenolphthalein indicator and a Fourier-transform infrared spectroscope (FTIR).

It was observed that the carbonation depth increases with w/c ratio, the age of concrete and the initial curing period. This difference in carbonation depths between air-cured and water cured samples was very small, with moist curing giving slightly lower carbonation depth. The discrepancy in the carbonation depth measured by IR for both air- and water-cured conditions reduced over time. Samples cured in water for 28 days became carbonated to only 53% of the level for air-cured samples but then increased to 78% after the three-month period (Lo and Lee, 2002). It was noted that 28-days strengths of moist cured samples were slightly higher.

In a critical review on the effect of curing on long-term natural carbonation of concrete, Ekolu, 2016 cited the long-term experimental studies by CSIR (Xue *et al.* 2015) and highlighted the fact that none of the curing regimes caused a change of strength class of a given mixture or any change in their respective carbonation behaviours under outdoor exposure (Table 2). In this study, it was observed that, for each strength class, the carbonation depths at later ages differ by about ±2 mm, regardless of the curing regime. Statistical analysis was conducted to assess whether the concretes subjected to the different curing regimes exhibited a significant change in carbonation. 95% confidence limit graphs were plotted. The residuals fell within the 95% confidence interval, indicating the absence of statistically significant differences between results of the various curing regimes. It was concluded that if a curing method causes a change in the strength class of a mixture then the corresponding carbonation behaviour of the mix can be expected to alter significantly.

Table 2. Results of carbonation depth using Phenolphthalein test and Infrared spectroscopic test

Mix (w/c)	Curing type	Strength (MPa)	Carbonation depth (mm) Phenolphthalein P Infrared spectrum (I)		
Age (month)			1	2	3
A (0.38)	Air	66	1 (1.5)	3.5 (4.5)	5 (6)
	Water	78	0.5 (1)	1.5 (3)	3 (4.5)
B (0.46)	Air	44	1.5 (3)	4 (6)	7 (8)
	Water	63	1 (3)	2.5 (4.5)	5 (6)
C (0.54)	Air	35	3 (4.5)	5.5 (8)	10 (12)
	Water	54	1.5 (3)	4 (6)	8.5 (10)

Table 3. Properties of concrete used by Balayssac *et al.* 1995

Concrete	Cement	Cement content (C) (kgm^{-3})	Water/ Cement	Gravel /Sand	Characteristic Strength (MPa)
B1	CPJ45	300	0.65	1.00	25.1
B2	CPJ45	340	0.61	1.13	32.6
B3	CPJ45	380	0.53	1.13	37.8
B4	CPJ45	420	0.48	1.15	43.5
-	CPA55	250	0.73	0.92	26.4
-	CPA55	280	0.65	0.94	30.0
-	CPA55	300	0.59	0.96	35.0
-	CPA55	350	0.54	1.04	41.8
-	CLK45	340	0.61	1.17	24.9
-	CLK45	400	0.50	1.15	31.9

The initial curing period of concrete plays a significant role in the carbonation of concrete. When curing is conducted for the proper time, the susceptibility of concrete to carbonation reduces. The purpose of curing is to maintain a required range of moisture and temperature.

An experimental study was conducted by (Balayssac *et al.* 1995) using concrete mixes of a range

of strength from 25 to 40 MPa. All mixes provided the same slump (8 cm). Cement content, w/c ratios and 28-day strengths are given in Table 3 and oxide composition and physical properties of cement are given in Table 4.

Table 4. Oxide composition and physical properties of cement used in Balayssac *et al.* 1995

Cement	CPJ45	CPA55	CLK45
SIO_2	26.2	20.1	30.3
Al_2O_3	3.1	5.4	11.5
Fe_2O_3	3.2	3.2	-
CaO	58.9	63.2	45.2
MgO	0.6	2.2	4.75
SO_3	2.6	2.3	2.9
K_2O	-	1.22	0.76
Na_2O	-	-	0.6
Ss ($m^2 kg^{-1}$)	350	370	385
Density	3.01	3.15	2.93

After demoulding at one day, the test samples were stored in a controlled environment (20 °C and 60% relative humidity) or kept in water up to 3 or 28 days, before exposure to the environment (with CO_2 content of 0.03%), for up to 18 months. Cylinders with 11 cm diameter and 10 cm height were used in this study whose ends were sawn after demoulding. Also, after curing, the lateral surfaces were covered with aluminium sheets. After an appointed period (90, 180, 360 and 540 days), three test samples were split to obtain a break without wet sawing. The carbonated depth was measured using phenolphthalein solution.

Carbonation depth decreased with an increase in cement content for any curing time (28-day strength). For the concrete with a cement content of 350 kgm^{-3}, increasing the period of curing from 1 day to 28 days caused the reduction of the carbonation depth to half. When the curing period was increased from 1 to 3 days, there was a rapid decrease in carbonation depth followed by slower variations. It was noted if cement content was too low, carbonation depth was still high in spite of good curing; also, curing effects depend on cement type. Increasing the curing period did not have the same effect, for the same cement content on the concrete of Portland Cement, as on the concrete of slag cement. One day curing was found to be insufficient for all the concretes, regardless of the cement content. In conclusion, curing for 3 days was sufficient for concretes with a cement content higher than 380 kgm^{-3} for good carbonation resistance. Detailed data on carbonation depths obtained are given in Table 5. Although some statistical and machine learning-based models are present (Taffese *et al.* 2015; Hills *et al.* 2015; Kwon and Song 2010; J.-K. Kim and Lee, 1999), analytical models involving the curing process were found to be very rare. The FIB-model (FIB 2006) accounts for the effect of site curing by providing a correction factor, which is dependent on the length of curing, but it does not mention anything on implications of different curing methods on natural carbonation (Ekolu, 2016).

3.2 Ambient Temperature and Thermal Properties

Small variations in temperature have little effect on carbonation. High temperature increases the carbonation rate unless drying overcomes the temperature effect (Neville, 1995). It also affects the passivity of steel rebars in reinforced concrete. Although the thermal conductivity of concrete is a well-researched topic because of its importance in fire-resistant design and energy conservation, its variation during carbonation of cement materials has not been studied to a good extent. The heat of hydration of concrete or occurrence of temperature gradient may lead to cracks in a concrete structure (Kim *et al.* 2003). Propagation of cracks increases the susceptibility of concrete to carbonation.

Table 5. Carbonation depths observed (Balayssac *et al.* 1995)

Concrete	Properties	Curing period	Age (days)			
			90	180	360	540
B1	Cement content=300 kg m^{-3}	1 day	6.5	11	13	15
	w/c =0.65	3 days	4	6	9.5	13
	28-day strength=25.1 MPa	28 days	3	5	6	9
B2	Cement content=340 kg m^{-3}	1 day	5.5	10	12	13
	w/c =0.61	3 days	3.5	5	6	8
	28-day strength=32.6 MPa	28 days	2.5	4	4.5	6
B3	Cement content=380 kg m^{-3}	1 day	4.5	9	10	11.5
	w/c=0.53	3 days	3	5	5.5	7
	28-day strength=37.8 MPa	28 day	2	3.5	4	5
B4	Cement content=420 kg m^{-3}	1 day	4	7.5	8.5	9.5
	w/c=0.48	3 days	2.5	4	3.5	4
	28-day strength=43.8 MPa	28 days	1.5	3	3	3.5

3.2.1 Effects of Ambient Temperature on Passivity Capacity of Reinforcement

Jiezhen (Hu *et al.* 2015) studied the coupled effect of temperature and carbonation on the corrosion of reinforcement by using the open circuit method (OCP), the electrochemical impedance spectroscopy (EIS) and the potentio-dynamic polarization (PP) in the simulated concrete pore solutions (SPSs). The OCP was used to evaluate the corrosion tendency of rebar in SPSs, the passivation film of the rebars was evaluated by using EIS and the corrosion current or dissolution velocity of the passivated surface of the rebars was evaluated using potentio-dynamic polarization measurements.

Following observations were made:

- The effect of temperature and pH on OCP: The rebars were found to be prone to corrosion in higher temperature and lower pH SPSs. The corrosion of rebar was high at pH = 9.6 and 318 K temperature of SPSs. The rebars had the best corrosion resistance at pH= 10.6 and 318 K temperature of SPSs.

- The effect of temperature and pH on Passivation Film of Rebar: The rebars were found to have a greater capacity of passivity at a lower temperature. Moderate pH value (11.6) SPSs was found to be favourable for the passivation layer.

- The effect of temperature and pH on the Corrosion Current of Rebar: The passive current of rebars in the higher pH value SPSs was bigger than that of rebars in lower pH value SPSs. This means that the dissolution velocity of the passivated surface is bigger if the pH of the SPSs is very high. Also, the high temperature and high pH environment are favourable for the formation of the passivated surface.

In conclusion, the high-temperature environment is favourable for the formation of the passivated surface of rebars in the SPSs; but the dissolution velocity of the passivated surface is higher in the high-temperature SPSs. Also, rebars have a greater capacity of passivity at a lower temperature. The corrosion rate of rebars at higher temperature is smaller in moderate pH value (10.6) SPSs. The rebars suffer from serious corrosion in pH= 9.6 SPSs at (high) 318 K temperature.

For a service life model for Reinforced concrete, it is very important to monitor the change in the pH of the pore solution. As discussed above, the onset of corrosion as well as the degree of corrosion is highly dependent on the pH of the pore solution. As per (Papadakis, Fardis, *et al.* 1991) the pH of carbonated concrete can be written as Eqn. (4):

$$pH = 14 + \log\left(2\times10^{3}\right)\left[Ca\left(OH\right)_{2}\right]_{aq} \quad (4)$$

As per the best knowledge of the authors, most of the models available for service life prediction of reinforced concrete doesn't consider the effect of temperature on the passivity of rebars. The threshold value pH for the onset of corrosion is dependent upon the temperature.

3.2.2 Effects of Sudden Changes in Temperature

According to S.K. Roy (Roy *et al.* 1999) the concrete structures which are exposed to the environment, faces not only seasonal and long-term changes in temperature but also sudden changes due to rain or change in temperate during day and night cycle. When there is a sudden fall in temperature, the outer concrete surface contracts more than the inside and tensile stress occur at the surface and compressive stress inside. Also, while the temperature rises suddenly, the outer surface of concrete expands more than the inside and compressive stresses develop at the surface and tensile stresses develop inside. This may lead to the formation of microcracks in concrete structures, increasing the surface area exposed to CO_2, leading to an increase in carbonation.

3.2.3 Effects on Thermal Conductivity

There is a good agreement to the fact that carbonation causes a reduction in the total porosity of concrete and alters its pore size distribution. The overall effect is that carbonation tends to increase the thermal conductivity appreciably (Pham and Prince 2013).

The thermal conductivity of concrete is a function of mix properties, types of aggregates used, as well as moisture status (Neville, 1995; Lanciani *et al.* 1989). Higher w/c ratios give a more porous structure. The pores have low thermal conductivity and heat capacity compared to the other phases present in concrete. More porosity enables a better scope for the influence of moisture content on the heat capacity of concrete. The moisture in any form in concrete, i.e., chemically bound, physically bound or free water, have higher heat capacity.

The changes in the micro-structure and macro-physical properties caused by the carbonation of normalised CEM II mortar were examined in detail Pham and Prince, 2013. Normalized mortar prepared with French Cement CEM II / BM (V-LL) 32.5 R and standard sand certified in accordance with EN 196-1 were used. The w/c and sand/cement ratios were respectively 0.5 and 3. At the end of the mixing, the mortar was placed in cylindrical moulds (diameter = 40 mm; height = 60 mm). The samples were demoulded after 24 h and then cured for 90 days in a humid chamber (20 °C, 100% RH). Samples were subjected to accelerated carbonation at

20°C, 65% RH and 20% CO_2 concentration. A Hot Disk Thermal Constants Analyser was used to perform the thermal conductivity test at 20 °C. The plane hot disk sensor was fixed between two pieces of the sample - each one with a plane surface facing the sensor. The hot disk sensor had a dynamic role. The disc was used both as a heat source and as a dynamic temperature sensor. Electrical current, high enough to increase the temperature of the sensor, was passed. The increase in resistance (temperature) was recorded as a function of time. Fig. 1 presents the variation of thermal conductivity during carbonation. The study confirmed that the thermal conductivity increases with an increase in carbonation.

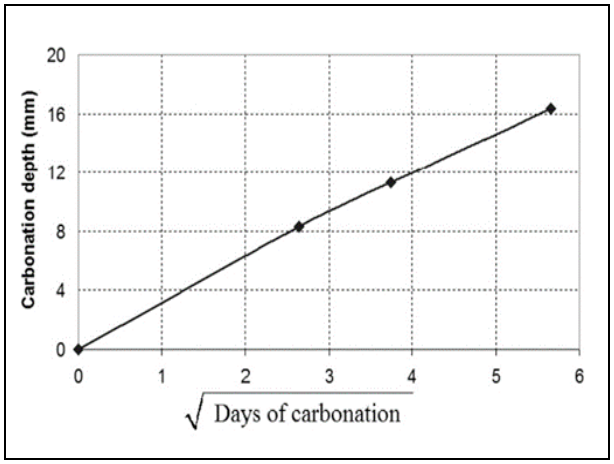

Fig. 1: Evolution of thermal conductivity with carbonation; Source: (Pham and Prince 2013)

3.2.4 Modeling of Heat Flow in Concrete

The modelling of heat flow inside concrete can be done using Fourier's law (Burkan Isgor *et al.* 2004), given by Eqn. (5),

$$-\frac{\partial}{\partial x}\left(-k\frac{\partial T}{\partial x}\right)-\frac{\partial}{\partial y}\left(-k\frac{\partial T}{\partial y}\right)+Q=\rho c\frac{\partial T}{\partial t} \quad (5)$$

where, k is the thermal conductivity of concrete ($Wm^{-1}°C$), T is its temperature (°C), ρ is its density ($kg\ m^{-3}$), c is its specific heat ($Jkg^{-1}°C$), t is time (s) and Q is the heat source/sink term. The procedure to find out the value of respective terms can be found out in the reference (Burkan Isgor *et al.* 2004). The boundary conditions at the concrete surface were found by considering total radiation absorbed, re-radiation by concrete, heat loss by convection and heat conducted into the concrete body. In this study, the thermal conductivity, k, and specific heat, c, which depend on the moisture content of the medium and degree of carbonation, were kept constant. The variations in their values were not considered to be significant for the normal temperature range.

In a study by (Shafei *et al.* 2012) Eqn. (5) was solved for a concrete member in a Finite Element framework. The developed finite-element model of the concrete member was subjected to the transient thermal analysis using the ANSYS program. To introduce the initial and boundary conditions, ambient temperature data was gathered for the specific region where the RC member was located. The daily temperature data of the study area was obtained for the last 15 years from the database. A sinusoidal curve (Eqn. 6), was fitted to the data:

$$T_{env}(t)=291-15\sin\left(\frac{2\pi t}{365}\right) \quad (6)$$

where, time, t is in days ($0\leq t\leq 365$). The boundary conditions were applied to the top and bottom surfaces of the concrete member. It was assumed that the temperature at the top surface follows the trend of Eqn. (6) over time. The bottom surface of the member also has the same trend with the half-variation amplitude. Based on the discussed assumptions and equations, the transient thermal analysis was performed on the finite-element model to calculate the temperature distribution in the nodes and elements of the concrete member. The temperature data was stored at each time step and then used as initial conditions for the next time step of the analysis.

3.3 Carbonation and Porosity of Concrete

As carbonation proceeds from the outer surface into internal portions of concrete, the micro-structure also changed continuously from the outer surface into internal portions of concrete (Song *et al.* 2007), consequently changing the porosity of the concrete. As $CaCO_3$ occupies a greater volume than $Ca(OH)_2$, which when it replaces, the porosity is reduced with the advancement of carbonation (Papadakis *et al.* 1991b; Burkan Isgor *et al.* 2004). Higher porosity gives rise to more carbonation, and this has been verified experimentally in a study by (Valcuende *et al.* 2010). Natural carbonation of self-compacting concrete was investigated in this study. Eight different concretes were used, which consisted of four self-compacting concretes (SCC) and four normally-vibrated concretes (NVC). The carbonation rate was found to be lower in SCC than NVC. It was attributed to the fact that limestone fines produce less porosity and finer micro-structure of concrete. Also, the difference between both types of concrete were tending to disappear as their fines content became similar.

In a study by Roy *et al.* 1999, the relationship between carbonation and the nature of the pores in the concrete was studied in detail. Larger pores gave rise to higher carbonation depths. Twenty concrete panels were cast and cured for 28 days and kept in two different locations for 2 years. Upon completion of the process, the median pore diameter was determined. Fig. 2 shows that the median pore diameters for the unmolded samples

(with large carbonation depth) are greater than those of the moulded samples (smaller carbonation depth). The result is presented in Fig. 2, which has shown the carbonation depth with the median pore size; a higher carbonation depth for increased pore size is also expected since a higher porosity will produce a higher diffusion rate for carbon dioxide. The importance of uniform and well-compacted concrete is also demonstrated since badly compacted or honeycombed concrete leads to high porosity and rapid carbonation.

The pore-blocking (due to rain) in concrete also influences the carbonation and hence it should also be accounted for in a concrete porosity model. The depth profiling of carbonates formed during natural carbonation of mortars with one face exposed directly to rain and opposite face sheltered has been measured and compared (Houst *et al.* 2002). Due to pore blocking by periodic rainwater, the amount of carbonates formed on mortars sheltered from the rain was found to be generally higher, as expected and explained by Papadakis *et al.* 1991a.

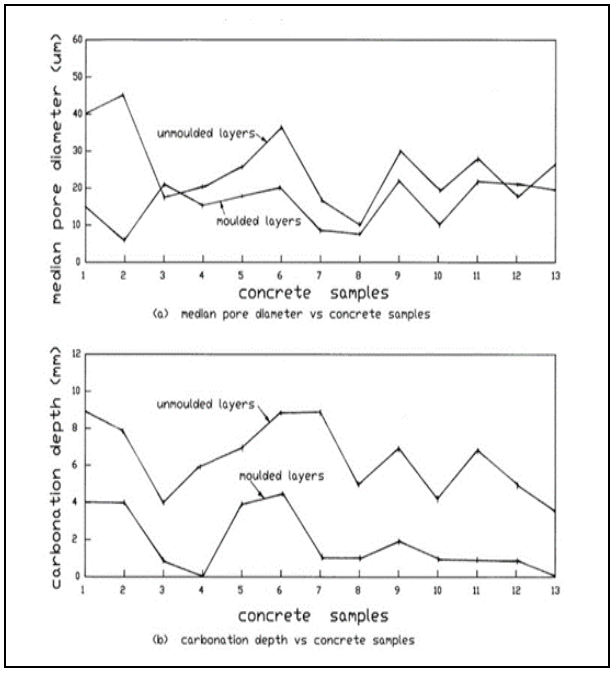

Fig 2: Median pore diameter and carbonation depth against concrete samples for moulded and un-moulded layers; Source: Roy *et al.* 1999

A practical method to find the initial porosity of concrete can be described as in Song *et al.* 2007. The permeability coefficient in carbonated concrete was derived by applying a capillary pore structure formation model in carbonated cement mortar and assuming that aggregates do not affect the carbonation process in early-aged concrete as a function of porosity. The permeability obtained from the micro-level modelling for carbonated concrete was verified with the results of the accelerated carbonation test and water penetration test in cement mortar. In this study, the permeability coefficient was obtained by Darcy's Law and the water flow in the unit time given is by Eqn. (7),

$$\frac{Q_f}{dt} = -\frac{A'dH}{dt} = \frac{K_p HA}{L} \tag{7}$$

$$-\frac{dH}{H} = \frac{K_p A dt}{A'L} \tag{8}$$

where, Q_f is total water flow, Q_f/dt is flow rate, A is the area of cement mortar, A' is the area of pipette attached to upside cell, L is the thickness of specimen, K_p is permeability coefficient and H is the water head. By integrating Eqn. (8) from the initial water head, H_0, to measured water head, H_1, as equation 9, the permeability coefficient Kp was obtained (Eqn. 9 and Eqn. 10).

$$-\int_{H_0}^{H_1} \frac{dH}{dt} = K_p \int_0^t \frac{Adt}{A'L} \tag{9}$$

$$K_p = \frac{A'L}{At} ln \frac{H_0}{H_1} \tag{10}$$

The relationship between carbonation and reduction in porosity has also been studied by Papadakis *et al.* 1991b, and for a fully hydrated concrete, it is given as Eqn. (11),

$$\mu(t) = f_d(t,\varphi)\mu_0 \tag{11}$$

where, $\mu(t)$ is the porosity of concrete at time t, $f_d(t,\varphi)$ is a decay function which may be used to determine the changed porosity of concrete due to carbonation, φ is the degree of carbonation and μ_0 is the initial porosity of concrete. A bi-linear decay function, as shown in Fig. 3, was used to simulate the effect of carbonation on the porosity. The parameters a and b in can be empirically determined. These are based on observed changes in porosity due to carbonation.

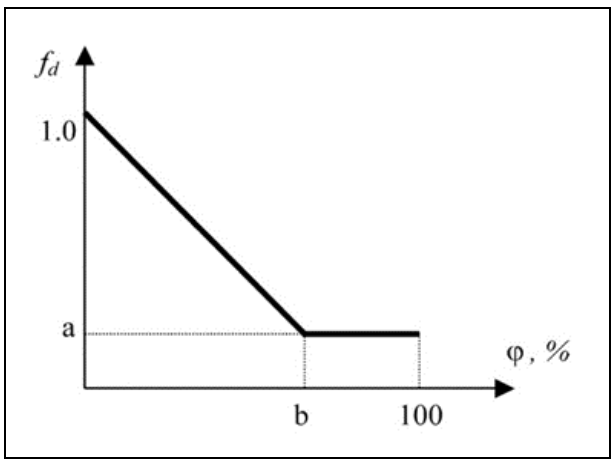

Fig 3: Decay function as a function of the degree of carbonation by (Papadakis *et al.* 1991b).

The initial porosity of concrete, μ_0, can be calculated using Eqn. (12),

$$\mu_0 = \frac{\frac{w}{c}\frac{\rho_c}{\rho_w}(1-\mu_{air})}{1+\frac{w}{c}\frac{\rho_c}{\rho_w}+\frac{a}{c}\frac{\rho_c}{\rho_a}} + \mu_{air} \quad (12)$$

where, for a given concrete, a/c is the aggregate–cement ratio, w/c is the water-cement ratio, μ_{air} is the air content of the concrete and ρ_c, ρ_a and ρ_w are the densities of cement, aggregates and water, respectively.

3.4 CO_2 Diffusivity

Bjorn Lagerblad (Lagerblad *et al.* 2005) stated that diffusion coefficient depends on microclimatic factors, essentially RH inside the cement paste and therefore, calculation of CO_2 uptake largely depends on laboratory testing and empirical data, including measurements on real concrete structures.

The transport of CO_2 inside concrete is governed by the following Eqn. (13) (Burkan Isgor *et al.* 2004), which is analogous to Eqn. (5).

$$\frac{\partial}{\partial x}\left(D_c\frac{\partial C_c}{\partial x}\right)+\frac{\partial}{\partial y}\left(D_c\frac{\partial C_c}{\partial y}\right)+Q_c=\frac{\partial C_c}{\partial t} \quad (13)$$

where, D_c (m^2s^{-1}) is the CO_2 diffusion coefficient, C_c (kgm^{-3} pore solution) is the CO_2 concentration, and Q_c ($kgm^{-3}s^{-1}$) is a sink term representing the reduction in the CO_2 content of concrete due to carbonation reaction (as discussed in Section 2). Papadakis (Papadakis *et al.* 1991b) proposed D_c, as a function of several factors such as temperature, relative humidity, age of concrete and exposure conditions (Eqn. 14).

$$D_c = 1.64\times10^{-6}\mu_p(t)^{1.8}(1-h)^{2.2} \quad (14)$$

where, h is the relative humidity, expressed as a fraction, at time t and $\mu_p(t)$ is the porosity of the hardened cement paste. The above expression has been used by (Burkan Isgor, *et al.* 2004) for their model for the prediction of concrete carbonation.

Another model proposed by Shafei (Shafei *et al.* 2012) used Eqn. (15) for the calculation of the CO_2 diffusion coefficient. They considered the effect of major influential factors such as ambient temperature $F_{B1}(T)$, relative humidity $F_{B2}(H)$, age of the concrete $F_{B3}(t_e)$, and change of the concrete pore structure during the carbonation process $F_{B4}(R)$ and the reference CO_2 diffusion coefficient $D_{B,ref}$.

$$D_B = D_{B,ref}F_{B1}(T)F_{B2}(H)F_{B3}(t_e)F_{B4}(R) \quad (15)$$

The values suggested by (Saetta, *et al.* 1995) were used for the calculation of different terms in Eqn. (15). The reference CO_2 diffusion coefficient for a normal strength concrete in the standard temperature and RH of 65% can be calculated using Eqn. (16):

$$D_{B,ref} = D_{B0}10^{-0.05f'cm} \quad (16)$$

where, f'_{cm} is the mean value of the 28-day compressive strength of the concrete (MPa) and D_{B0} is equal to $10^{-6.1}$ m^2s^{-1}.

$$F_{B2}(H) = (1-H)^{2.5} \quad (17)$$

where, H is the corresponding pore relative humidity.

$$F_{B1}(T) = exp\left[\frac{E}{R}\left(\frac{1}{T_{ref}}-\frac{1}{T}\right)\right] \quad (18)$$

where, R is the gas constant (kJ (mol. K)$^{-1}$), and E is the activation energy of diffusion process ($kJmol^{-1}$). The value of E for a cement paste made of OPC depends on the water to cement ratio.

$$F_{B3}(t_e) = \chi+(1-\chi)\left(\frac{28}{t_e}\right)^{0.5} \quad (19)$$

where, t_e is the age of the concrete (day) and χ is the ratio of the diffusivity at the time of diffusivity to the diffusivity after 28 days.

$$F_{H4}(R) = 1-\varepsilon R \quad (20)$$

where, the value of ε ranges between 0 and 1. If the diffusion process results in no reduction in porosity, ε will become zero. R is the degree of carbonation. The degree of carbonation is determined as the ratio of accumulated CO_2 already reacted with $Ca(OH)_2$ to the maximum possible concentration of reacted CO_2 in the concrete. Further details about these parameters can be read in detail in reference (Shafei *et al.* 2012).

3.5 Carbonation of Concrete Containing Blended Cements

Blended cements have widespread use and different types of cements have very different micro-structural and physical properties. Thus, it is essential to understand the nuances of carbonation properties of different hardened cement paste made up of Pozzolana cement, ground granulated blast furnace, slag cement, etc. The effect of supplementary cementing materials (SCM) on concrete resistance against carbonation and chloride ingress has been studied by Papadakis, 2000. The silica fume and low and high calcium fly ash were used as SCM. Experimental investigations simulating main deterioration mechanisms in reinforced concrete were carried out. It was observed that the carbonation

depth decreased with increase in aggregate replacement by SCM and increased as cement replacement by SCM increased.

3.5.1 Carbonation of Cement containing Fly Ash

It has been reported that the normal dosages of fly ash addition result in a slight increment of the carbonation of concrete, whereas in concrete with normal moist-curing periods, carbonation is not affected by the significant amount. Many studies have reported that higher carbonation has been found in concrete containing fly ash (Ho *et al.* 1987, 1988; Thomas *et al.* 1990; Papadakis *et al.* 1992; Atiş *et al.* 2003; Sulapha *et al.* 2003). Contrary to these studies, in a case where a 25-year-old fly ash foundation concrete was examined, and it has been reported that there has been no carbonation in the fly ash concrete specimens. (Cabrera and Woolley, 1985). The study by (Thomas *et al.* 1992), concludes that concretes with up to 30% fly ash carbonated to a similar or slightly greater degree compared with OPC concretes of the same strength grade. However, concretes containing 50% fly ash carbonated at significantly greater rates. This study reports carbonation of fly ash concrete, with particular emphasis on the role of curing. It also observes that in some cases, increasing the initial curing period from 1 to 7 days had the effect of reducing carbonation by 50%. Concretes with nominal strength grades M25, M35 and M4.5 and a range of fly ash levels (0-50%) were exposed to various treatments and environment during the first 28 days. After 28 days, the concrete cubes were stored either internally or externally (sheltered) and the rate of carbonation was monitored.

Papadakis (Papadakis *et al.* 2000) reported that fly ash is introduced in the casing as a fine aggregate replacement, the carbonation rate is reduced. (Khunthongkeaw *et al.* 2006) However, reaction products between pozzolanic silica and $Ca(OH)_2$ result in the denser structure of the HCP, so diffusivity is reduced and carbonation is likely to be slowed down. For this to happen, good curing is essential (Parrott *et al.* 1987; Hobbs *et al.* 1988).

3.5.2 Carbonation of Concrete Containing Silica Fume

A study by (Kulakowski *et al.* 2009) signifies the conclusions regarding the depth of carbonation; carbonation induced reinforcement corrosion in concrete samples with silica fume addition upto 20% and the water/binder ratios ranging from 0.30-0.80. The water-binder ratios specify the behaviour of the additions. In the materials having w/b ratios lower or equal to 0.45-0.50, the porosity of the material is the governing factor in the process of carbonation, whereas the consumption of the calcium hydroxide has an insignificant effect on the carbonation. On the contrary, for higher w/b ratios, a substantial role is played by the consumption of calcium hydroxide. At the same time, the results concluded from the reinforcement corrosion studies direct that the outcome of the silica fume addition is to be governed by their concentration. Silica fume will not lessen the corrosion resistance for the concentrations equal to or lower than 10% and it might actually increase it when used in the concentrations below this level. Silica fume increases the potential for carbonation-induced reinforcement corrosion when used in concentrations greater than 10%.

3.5.3 Carbonation of Concrete containing Alkali-Activated Blast-Furnace Slag Mortar (AAS)

Different studies on Alkali-Activated Blast-Furnace Slag Mortar (AAS) have shown that AAS has lesser resistance to carbonation (Song *et al.* 2014; Cabrera and Woolley, 1985). Unlike OPC, the compressive strength of AAS reduces. This can be attributed to the fact that the major hydration product of AAS is calcium silicate hydrate (CSH), with almost no portlandite, unlike the products of OPC. After carbonation, the CSH of AAS turned into amorphous silica gel and hence, reducing the compressive strength; also, the increase of the activator dosage leads AAS to react more quickly and produce more CSH, increasing the compaction, compressive strength and carbonation resistance of the microstructure (Song *et al.* 2014).

3.5.4 Carbonation of Concrete containing Granulated Blast Furnace Slag Cement (GBFSC)

G. G. Litvan and A. Meyer (Litvan *et al.* 1986) carried out a long-term study to illustrate the comparison of carbonation between granulated blast furnace slag cement (GBFSC) concrete and ordinary Portland cement (OPC) concrete. It was found that the rate of carbonation in GBFSC significantly surpasses when compared to the rate in OPC concrete. Declination has been shown in the porosity of OPC concrete, whereas in the case of GBFSC, it remained the same. The basic source of the increase in the permeability of GBFSC concrete with carbonation was the coarsening of the pores, and a large decrease was suffered by the tensile strength of the surface region.

Although lots of experimental work has been done, research work performed on the carbonation prediction of the concrete containing SCMs are rare.

Jiang (Jiang *et al.* 2000) developed a mathematical model (Eqn. 21) to predict carbonation depth of High-volume Fly Ash (HVFA) concrete. In this study, an accelerated carbonation test was carried out on Ordinary Portland Cement (OPC) concrete and HVFA concrete.

$$X_C = 839(1-RH)^{1.1}\sqrt{\frac{\left(\frac{W}{B^*}-0.34\right)C_o}{\propto k'C}}\sqrt[2]{t} \qquad (21)$$

where, W/B^* =effective w/c ratio, $\propto$ is the degree of hydration, C_o = concentration of CO_2, C = cement content, k'= coefficient related to carbonation reactivity depending on the contents of cement and fly ash, n is a parameter related to the pore system of concrete (reported to have a value between 2.0 and 2.1). The predicted depth results were compared with the experimental results. Researchers also pointed out that the effective water/binder ratio and the cement content are the important parameters influencing HVFA concrete carbonation.

Wang (Wang *et al.* 2009) suggested a multi-component concept-based numerical model which can predict the carbonation of concrete containing silica fume. This numerical model had two parts: hydration and carbonation models. The hydration model takes the mixed proportion of concrete as input and considers Portland cement hydration and pozzolanic activity. From the model, the amount of hydration product that is susceptible to carbonate along with porosity was obtained as a function of curing age. The diffusivity of CO_2 in concrete was also determined and the carbonation depth of concrete was also predicted. The prediction results showed a good agreement with the results of the experiment performed in this study.

3.6 Effects of Water/Cement Ratio

The water/cement (w/c) and water/binder ratio are considered as one of the most important design parameters affecting concrete quality. It has been verified by several studies (Fattuhi *et al.* 1986; Roy *et al.* 1999; Chaussadent *et al.* 2000) that the depth of carbonation increases with an increase in water/cement ratio. This is attributed to the strong influence of the w/c ratio on the microstructural properties of concrete. The effect of the water-cement ratio of cement pastes on microstructural characteristics related to the carbonation process was studied by Chaussadent *et al.* 2000. Investigations were performed during the hydration process at an early age and on 28-day and 2-year-old hydrated cement pastes. The mix was made with Type I Normal Portland Cement. The w/c ratios used in this study were 0.25, 0.35, 0.45, and 0.60. It was observed that the microstructural characteristics are very different between pastes having w/c values above 0.35-0.40 and below 0.35-0.40. When w/c is more than this value, the porosity strongly increases and the calcium hydroxide appears in large crystals. It was also observed that, for an equivalent degree of hydration, the calcium hydroxide amount increases and the CaO/SiO_2 ratio of the $C-S-H$ decreases as the w/c increases.

An experimental study (Roy *et al.* 1999) to understand the effect of water-cement ratio on carbonation has been conducted using w/c ratios of 0.55, 0.60, 0.65, 0.70 and 0.75. The cubes were cast and their compressive strengths were measured after 28 days of curing; another prism cast of the same sample was cured for 7 days and transferred to the carbonation chamber and its carbonation depth wase measured on weekly basis for 6 weeks. The data of carbonation depth are summarized in Table. 6 It has been observed that samples having higher w/c ratios which are of a lower grade of concrete shows larger carbonation depths. The rate constant, K (mm/year $^{0.5}$) were calculated on the basis of carbonation depths, assuming carbonation as a diffusion-controlled phenomenon and the carbonation depth d (in mm), is correlated to the exposure time, t (years) by Eqn. (22):

$$d = K\sqrt{t}^{0.5} \quad (22)$$

The calculated K-values are shown in Table 6; it has been observed that K increased with increase in w/c ratio or decrease in cube strength. A similar relationship between concrete strength (grade, quality) and carbonation rate has been quite well established in several previous studies.

It was concluded that there exists a relationship between the rate (depth) of carbonation and the strength of the concrete sample. The carbonation depth was found to be proportional to (strength)$^{-1}$ and the carbonation rate constant, K (mm year)$^{0.5}$, measured in the accelerated laboratory tests, were significantly higher than those found in normal atmospheric conditions.

Similar results were also obtained in the study by Fattuhi *et al.* 1986. Accelerated carbonation technique was used to investigate the effects of concrete mix w/c ratio on the rate of concrete carbonation. Prisms (50 x 50 x 285 mm) made from concretes with w/c ratios of 0.7, 0.6 and 0.4. The prisms were initially water cured for 1, 3, 7, 21 or 28 days; then they were placed in a chamber filled with CO_2 gas. The carbonation depth was examined using a phenolphthalein indicator. The results have shown that the depth of carbonation increased with an increase in the concrete w/c ratio.

3.7 Effect of Ambient Humidity and Moisture Content

Deterioration of the concrete may be caused by various chemical processes and water may act as an essential component in these reactions (Burkan Isgor *et al.* 2004). For lower relative humidity (RH less than 50%), diffusion of CO_2 into concrete is high, but there may not be enough water in the pores to support carbonation. For a high RH, diffusion of CO_2 is very low, which leads to a reduction in carbonation and its carbonation rate (Papadakis *et al.* 1991b; Papadakis *et al.* 1992; Castel *et al.* 1999); the reason why majority of the studies on concrete carbonation use RH between 50% and 70%.

Roy (Roy *et al.* 1999) conducted an experimental study to find the effect of humidity levels on the depth of carbonation and the author used five

different grades of concrete (Grade 20, 25, 30, 35 and 40 with w/c ratio of 0.8, 0.7, 0.65, 0.6 and 0.55 respectively). After curing for 28 days, the samples were transferred in special chambers having CO_2 at 6% by volume with humidity levels 52, 64, 75, 84 and 92%, to accelerate the carbonation process. Carbonation tests were carried out at five different exposure periods *viz*, 0, 1, 4, 8 and 16 weeks. From Fig. 4, it is visible that significant carbonation is visible only after 8 or 16 weeks. By looking at the carbonation depth *vs.* humidity level relationship after 16 weeks of exposure, the same general trends can be seen from all five grades of concrete. As the humidity level increases from 52 to 75%, there is a significant increase in carbonation depth. Then a decrease in carbonation depth was observed as the relative humidity increases from 75 to 84% before the carbonation depth increases once again as the relative humidity increases to further up to 92%.

Table 6: Cube strength, carbonation depths and carbonation rate constant for various grades of concrete

Water/cement ratio	Cube strength (MPa)	Carbonation depth (mm) after different exposure periods						Carbonation rate constant K (mm/year$^{-0.5}$)
		7	14	21	28	35	42	
0.55	27.0	0	1	2.2	3.0	3.7	5.3	10.89
0.60	26.5	0	1	2.8	3.3	4.5	5.5	11.89
0.65	23.5	0	1	3.3	3.8	5.1	7.1	13.7
0.70	20.5	0	1	3.9	4.3	6.1	7.5	15.5
0.75	18.5	0	1	4.1	4.7	6.3	8.5	16.9

Table 7. Details of mix used (Russell *et al.* 2001) (Fine aggregate/coarse aggregate ratio was held constant at 0.55)

Mix No.	w/c ratio	Cement content kgm^{-3}	Water content kgm^{-3}	Fine aggregate content kgm^{-3}	Coarse aggregate content kgm^{-3}	Achieved a/c ratio
1	0.50	375	192	685	1243	5.14
2	0.57	375	215	664	1207	4.99
3	0.63	375	234	647	1174	4.86
4	0.70	375	256	625	1140	4.71
5	0.50	315	164	732	1329	6.54
6	0.57	315	184	711	1296	6.37
7	0.63	315	201	696	1296	6.23
8	0.70	315	220	679	1233	6.07

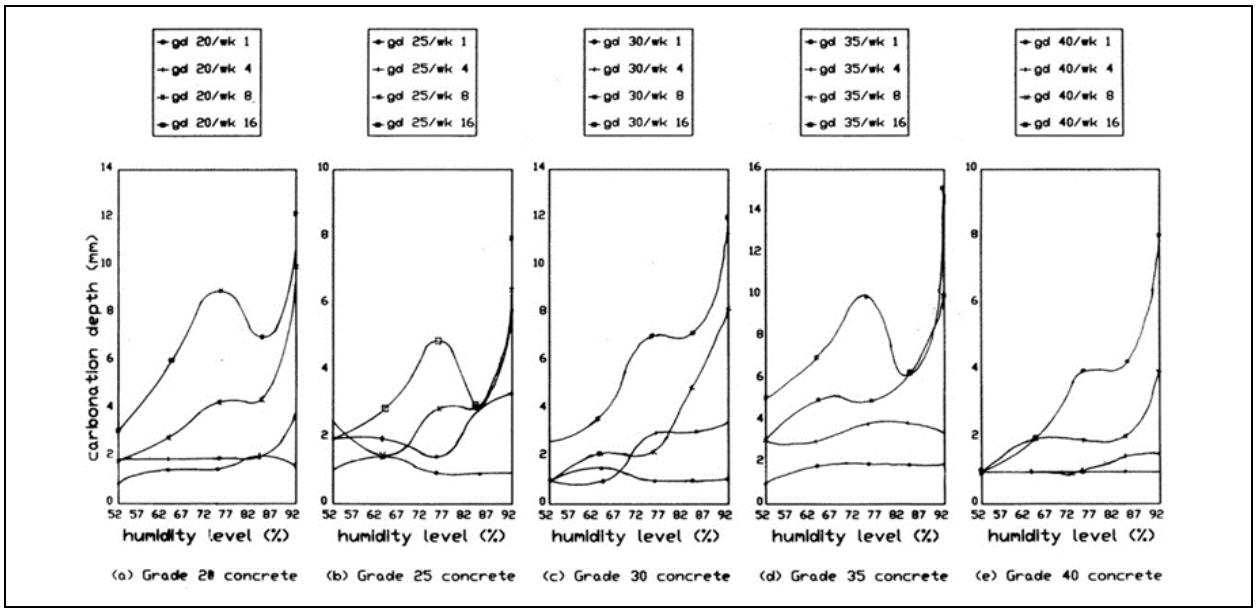

Fig. 4: Carbonation depth v/s Humidity level for different grades of concrete (Roy *et al.* 1999).

So, based on the experimental study, it can be concluded that the effects of RH were complex, with maxima being measured at both 75% and 92% RH. The former maxima were similar to real structures and the enhanced carbonation at latter maxima RH may be possible due to the difference in the mechanism(s) of carbonation in the accelerated depths (Roy *et al*. 1999).

Russell *et al.* 2001 conducted a study to investigate the effect of relative humidity on the rate of carbonation. Based on the data from an accelerated carbonation test, descriptive models were developed to quantify the effects of relative humidity on the rate of carbonation. Eight different concrete mixes were used. Four different w/c ratios and two cement contents (CC) were used. Three batches of these eight mixes were cast for testing at three different RH conditions: 55, 65 and 75% RH. All other properties like curing, conditioning and exposure to the CO_2 environment were held constant for all the mixes. Details of the eight mixes used in the test are given in Table 7. Class 42.5 N Portlnd cement (OPC) conforming to BS12: 1991 was used. The carbonation chamber was set to maintain a 5% CO_2 ($\pm$ 0.5%) concentration at 20˚°C ($\pm$1°C) during the testing. Carbonation was measured using 1% phenolphthalein solution. Internal humidity was monitored at 0, 10, 20, 30 and 40 mm depths from the exposed surface.

The rates of carbonation of all mixes are given in Table 8 using Eqn. 22. The overall trend observed was that the rate of carbonation decreased with increase in RH. For the lower w/c ratio mixes, the greatest change in the rate of carbonation occurred between 55% and 65% target RH. Maximum carbonation occurred at 55–65% RH. From 65 to 75% RH, there was a decrease in the rate of carbonation.

Table 8: Carbonation rates obtained for different values of RH (Russell *et al.* 2001)

w/c ratio	Cement content kgm^{-3}	Target relative humidity		
		55%	65%	75%
		Carbonation rate mm/week$^{0.5}$		
0.50	375	3.32	1.43	1.97
0.57	375	5.56	2.90	2.39
0.63	375	5.49	6.08	3.06
0.70	375	9.84	7.94	2.74
0.50	315	4.40	1.71	1.32
0.57	315	4.48	4.20	2.42
0.63	315	8.72	6.34	2.82
0.70	315	10.96	7.62	4.18

4. CONCLUSION

A review has been presented with the aim of examining the effects of different parameters influencing the carbonation of concrete. Further, uncertainties, similarities and dissimilarities across different experimental studies have been discussed. Also, insights have been given on different analytical and empirical models developed so far. The following findings are reported:

I. Carbonation is a multi-variable and non-linear phenomenon. The factors influencing the carbonation of concrete are interdependent and the entire process is highly complex. Thus, modelling for the prediction of concrete carbonation should be based on the non-linear scheme. Non-linear FEM-based models performed satisfactorily for carbonation depth prediction. Several neural network-based models have also been developed. Because of non-linear and interdependent nature of the problem, ANN, GA and other artificial intelligence-based models can be deployed effectively.

II. Equation 2, which defines a linear relationship between carbonation depth and the square root of time with a proportionality constant, has been used by several researchers for reporting the effects of influencing parameters on the carbonation of concrete. This equation considers diffusion properties to be constant, which does not reflect a real scenario. Also, as observed across different experimental data the proportionality constant changes appreciably. Although highly convenient in comparing results in controlled laboratory conditions, this equation should not be used to study or predict long-term natural carbonation of concrete.

III. Carbonation resistance of concrete increases with an increase in the curing period. Different curing regimes do not affect carbonation until it causes a change in the characteristic strength of concrete. Curing period of three days is sufficient for developing good carbonation resistance in concrete.

IV. The high-temperature environment was found to be favourable for the formation of the passivated surface of rebars in the SPSs. But the dissolution velocity of the passivated surface is also higher in the high-temperature SPSs. Thus, the rebars have a greater capacity of passivity at a lower temperature.

V. In general, carbonation of concrete causes an increase in the thermal conductivity and all the mechanical properties of concrete like strength, modulus of elasticity and shrinkage of the concrete.

VI. Higher porosity gives rise to higher carbonation depths. To ensure lower porosity or denser structure, concrete should be uniform and well-compacted with high cement content. Carbonation causes a reduction in the porosity of the concrete. Therefore, carbonation slows down with time or its

propagation. Pore blocking due to rain may also influence carbonation propagation. Hence, in a porosity model, a function that incorporates initial concrete properties as well as other variables like degree of carbonation, relative humidity and temperature must be used.

VII. In general, the carbonation depth decreases as aggregate replacement by SCM increases and increases as cement replacement by SCM increases. Concretes with up to 30% fly ash carbonated to a similar or slightly greater degree compared with OPC concretes of the same strength grade. However, concretes containing 50% fly ash were found to carbonate at significantly higher rates.

VIII. The rate of carbonation was found to be increasing with an increase in the w/c ratio. The water-cement ratio is the most important parameter influencing the carbonation of concrete. Concretes having lower w/c ratios were found to be more carbonation-resistant even with smaller curing periods.

IX. With the increase in the humidity level from around 50% to 75%, there is a significant increase in carbonation depth; there is a decrease in carbonation depth with further increase in relative humidity from 75 to 84%.

FUNDING

This research received no specific grant from any funding agency in the public, commercial, or not-for-profit sectors.

CONFLICTS OF INTEREST

The authors declare that there is no conflict of interest.

COPYRIGHT

REFERENCES

Aprianti, E., Shafigh, P., Zawawi, R., Abu Hassan, Z. F., Introducing an effective curing method for mortar containing high volume cementitious materials, *Constr. Build. Mater*., 107, 365–377 (2016). https://doi.org/10.1016/j.conbuildmat.2015.12.100

Atiş, C. D., Carbonation-Porosity-Strength Model for Fly Ash Concrete, *J. Mater. Civ. Eng.*, 16(1), 91–94 (2004). https://doi.org/10.1061/(ASCE)0899-1561(2004)16:1(91)

Atiş, C. D., Accelerated carbonation and testing of concrete made with fly ash, *Constr. Build. Mater.* 17(3), 147–152 (2003). https://doi.org/10.1016/S0950-0618(02)00116-2

Baba, A., Senbu, O., A predictive procedure for carbonation depth of concrete with various types of surface layers, In: Proceedings of Fourth International Conference on Durability of Building Materials and Components. Singapore, pp 679–685

Balayssac, J. P., Détriché, C. H., Grandet, J., Effects of curing upon carbonation of concrete, *Constr. Build. Mater.*, 9(2), 91–95 (1995). https://doi.org/10.1016/0950-0618(95)00001-V

Broomfield, J. P., Corrosion of Steel in Concrete: Understanding, Investigation and Repair, Second Edition. Corrosion of Steel in Concrete: Understanding, Investigation and Repair, *Second Edition, Taylor & Francis*, (2006).

Burkan Isgor, O., Razaqpur, A. G., Finite element modeling of coupled heat transfer, moisture transport and carbonation processes in concrete structures, *Cem. Concr. Compos*., 26(1), 57–73(2004). https://doi.org/10.1016/S0958-9465(02)00125-7

Cabrera, J. G., Woolley, G. R., A study of twenty-five year old pulverized fuel ash concrete used in foundation structures, *Proc. lnstn Ciu. Engrs.*, 79(1), 149–166. https://doi.org/10.1680/iicep.1985.1085

Castel, A., François, R., Arliguie, G., Effect of loading on carbonation penetration in reinforced concrete elements, *Cem. Concr. Res.*, 29(4), 561–565 (1999). https://doi.org/10.1016/S0008-8846(99)00017-4

Chang, J. J., Yeih, W., Huang, R., Chi, J. M., Mechanical properties of carbonated concrete, *J. Chinese Inst. Eng.*, 26(4), 513–522 (2003). https://doi.org/10.1080/02533839.2003.9670804

Chaussadent, T., Hornain, H., Rafai, N. and Ammouche, A., V. B.-B., Effect of Water-Cement Ratio of Cement Pastes on Microstructural Characteristics Related to Carbonation Process, *Spec. Publ.*, 192, 523–538(2000). https://doi.org/10.14359/5769

Ekolu, S. O., A review on effects of curing, sheltering, and CO2concentration upon natural carbonation of concrete, *Constr. Build. Mater*. 127, 306–320 (2016). https://doi.org/10.1016/j.conbuildmat.2016.09.056

Ekolu, S. O., Heat curing practice in concrete precasting technology–problems and future directions, *Concr. Soc. South Africa.*, 114, 5–10. (2006).

Fattuhi, N. I., Carbonation of concrete as affected by mix constituents and initial water curing period, Mater. Struct. 19(2), 131–136 (1986). https://doi.org/10.1007/BF02481757

FIB, F. I. B., Model Code for Service Life Design, Int. Fed. Struct. Concr. (FIB). Switz. , 110 (2006). https://doi.org/10.35789/fib.BULL.0034

Hills, T. P., Gordon, F., Florin, N. H., Fennell, P. S., Statistical analysis of the carbonation rate of concrete, *Cem. Concr. Res*., 72, 98–107 (2015). https://doi.org/10.1016/j.cemconres.2015.02.007

Ho, D. W. S., Lewis, R. K., Carbonation of concrete and its prediction, *Cem. Concr. Res.*, 17(3), 489–504 (1987). https://doi.org/10.1016/0008-8846(87)90012-3

Ho, D. W. S., Lewis, R. K., The specification of concrete for reinforcement protection— performance criteria and compliance by strength, *Cem. Concr. Res*., 18(4), 584–594 (1988). https://doi.org/10.1016/0008-8846(88)90051-8

Hobbs, D. W., Carbonation of concrete containing pfa, *Mag. Concr. Res.*, 40(143), 69–78 (1988). https://doi.org/10.1680/macr.1988.40.143.69

Houst, Y. F., Wittmann, F. H., Depth profiles of carbonates formed during natural carbonation, Cem. Concr. Res., 32(12), 1923–1930 (2002). https://doi.org/10.1016/S0008-8846(02)00908-0

Hu, J., Cheng, X., Li, X., Deng, P., Wang, G., The Coupled Effect of Temperature and Carbonation on the Corrosion of Rebars in the Simulated Concrete Pore Solutions, *J. Chem.*, 462605(2015). https://doi.org/10.1155/2015/462605

Hussain, R. R., Enhanced mass balance Tafel slope model for computer based FEM computation of corrosion rate of steel reinforced concrete coupled with CO2 transport, *Comput. Concr*., 8(2), 177–192(2011). https://doi.org/10.12989/cac.2011.8.2.177

Jiang, L., Lin, B., Cai, Y., A model for predicting carbonation of high-volume fly ash concrete, *Cem. Concr. Res*., 30(5), 699–702 (2000). https://doi.org/10.1016/S0008-8846(00)00227-1

Khan, M. I., Lynsdale, C. J., Strength, permeability, and carbonation of high-performance concrete, *Cem. Concr. Res.*, 32(1), 123–131 (2002). https://doi.org/10.1016/S0008-8846(01)00641-X

Khunthongkeaw, J., Tangtermsirikul, S., Leelawat, T., A study on carbonation depth prediction for fly ash concrete, *Constr. Build. Mater*., 20(9), 744–753 (2006). https://doi.org/10.1016/j.conbuildmat.2005.01.052

Kim, J.-K., Lee, C.-S., Moisture diffusion of concrete considering self-desiccation at early ages, *Cem. Concr. Res*., 29(12), 1921–1927 (1999). https://doi.org/10.1016/S0008-8846(99)00192-1

Kim, K.-H., Jeon, S.-E., Kim, J.-K., Yang, S., An experimental study on thermal conductivity of concrete, *Cem. Concr. Res*., 33(3), 363–371 (2003). https://doi.org/10.1016/S0008-8846(02)00965-1

Kobayashi, K., Suzuki, K., Uno, Y., Carbonation of concrete structures and decomposition of C-S-H, *Cem. Concr. Res*., 24(1), 55–61 (1994). https://doi.org/10.1016/0008-8846(94)90082-5

Kulakowski, M. P., Pereira, F. M., Molin, D. C. C. D., Carbonation-induced reinforcement corrosion in silica fume concrete, *Constr. Build. Mater.*, 23(3), 1189–1195 (2009). https://doi.org/10.1016/j.conbuildmat.2008.08.005

Kwon, S.-J., Song, H.-W., Analysis of carbonation behavior in concrete using neural network algorithm and carbonation modeling, *Cem. Concr. Res.*, 40(1), 119–127 (2010). https://doi.org/10.1016/j.cemconres.2009.08.022

Lagerblad, B., Carbon dioxide uptake during concrete life cycle – State of the art, Carbon dioxide uptake during concrete life cycle – State of the art, Stockholm (2005).

Lanciani, A., Morabito, P., Rossi, P., Barberis, F., Berti, R., Capelli, A., Sona, G. S., Measurements of the thermophysical properties of structural materials in laboratory and in situ: Methods and instrumentation, *High Temp. - High Press.*, 21(4), 391–400 (1989).

Leemann, A., Nygaard, P., Kaufmann, J., Loser, R., Relation between carbonation resistance, mix design and exposure of mortar and concrete, *Cem. Concr. Compos.*, 62, 33–43 (2015). https://doi.org/10.1016/j.cemconcomp.2015.04.020

Litvan, G. G., Meyer, A., Carbonation of granulated blast furnace slag cement concrete during twenty years of field exposure, In: ACI SP. 1445–1462

Liu, Y., Zhao, S., Yi, C., The Forecast of Carbonation Depth of Concrete Based on RBF Neural Network, In: 2008 Second International Symposium on Intelligent Information Technology Application. 544–548.

Lo, T. Y., Liao, W., K. Wong, C., Tang, W., Evaluation of carbonation resistance of paint coated concrete for buildings, *Constr. Build. Mater*., 107, 299–306 (2016). https://doi.org/10.1016/j.conbuildmat.2016.01.026

Lo, Y., Lee, H. M., Curing effects on carbonation of concrete using a phenolphthalein indicator and Fourier-transform infrared spectroscopy, *Build. Environ.* 37(5), 507–514 (2002). https://doi.org/10.1016/S0360-1323(01)00052-X

Nagataki, S. and H. Ohga, M. A. M., Carbonation of Mortar in Relation to Ferrocement Construction, *Mater. J.*, ,85(1), 17–25 (1988). https://doi.org/10.14359/2475

Neville, A. M., Properties of concrete. Properties of concrete, Longman London, 1995.

Papadakis, V. G., Effect of supplementary cementing materials on concrete resistance against carbonation and chloride ingress, *Cem. Concr. Res*., 30(2), 291–299 (2000). https://doi.org/10.1016/S0008-8846(99)00249-5

Papadakis, V. G., Fardis, M. N., Vayenas, C. G., Fundamental Modeling and Experimental Investigation of Concrete Carbonation, *Mater. J.*, 88(4), 363–373 (1991a). https://doi.org/10.14359/1863

Papadakis, V. G., Vayenas, C. G., Fardis, M. N., Hydration and Carbonation of Pozzolanic Cements, *Mater. J.*, 89(2), 119–130 (1992). https://doi.org/10.14359/2185

Papadakis, V. G., Vayenas, C. G., Fardis, M. N., Experimental investigation and mathematical modeling of the concrete carbonation problem, *Chem. Eng. Sci*., 46(5), 1333–1338 (1991b). https://doi.org/10.1016/0009-2509(91)85060-B

Parrott, L. J., Carbonation, moisture and empty pores, *Adv. Cem. Res*., 4(15), 111–118 (1992). https://doi.org/10.1680/adcr.1992.4.15.111

Parrott, L. J., A Review of Carbonation in Reinforced Concrete. A Review of Carbonation in Reinforced Concrete, *Cement and Concrete Association*, (1987)

Pham, S. T., Prince, W., Effects of Carbonation on the Microstructure and Macro Physical Properties of Cement Mortar, World Acad. Sci. Eng. Technol. *Int. J. Civil, Environ. Struct. Constr. Archit. Eng.*, 7(6), 434–437 (2013).

Qiu-Dong, L. Y.-U. and W., Mechanism of Carbonation of Mortars and the Dependence of Carbonation on Pore Structure, *Spec. Publ*., 100, 1915–1944 (1987). https://doi.org/10.14359/3838

Roy, S. K., Poh, K. B., Northwood, D. o., Durability of concrete—accelerated carbonation and weathering studies, *Build. Environ*., 34(5), 597–606 (1999). https://doi.org/10.1016/S0360-1323(98)00042-0

Russell, D., Basheer, P. A. M., Rankin, G. I. B., Long, A. E., Effect of relative humidity and air permeability on prediction of the rate of carbonation of concrete, In: Proceedings of the Institution of Civil Engineers - Structures and Buildings. ICE Publishing, 319–326 (2001)

Saetta, A. V, Schrefler, B. A., Vitaliani, R. V, 2 — D model for carbonation and moisture/heat flow in porous materials, *Cem. Concr. Res*., 25(8), 1703–1712 (1995). https://doi.org/10.1016/0008-8846(95)00166-2

Šauman, Z., Carbonization of porous concrete and its main binding components, *Cem. Concr. Res*., 1(6), 645–662 (1971). https://doi.org/10.1016/0008-8846(71)90019-6

Shafei, B., Alipour, A., Shinozuka, M., Prediction of corrosion initiation in reinforced concrete members subjected to environmental stressors: A finite-element framework, *Cem. Concr. Res*., 42(2), 365–376 (2012). https://doi.org/10.1016/j.cemconres.2011.11.001

Shigeyoshi Nagataki and Eun Kyum Kim, H. O., Effect of Curing Conditions on the Carbonation of Concrete with Fly Ash and the Corrosion of Reinforcement in Long-Term Tests, *Spec. Publ*., 91, 521–540 (1986). https://doi.org/10.14359/10086

Slegers, P. A., Rouxhet, P. G., Carbonation of the hydration products of tricalcium silicate, *Cem. Concr. Res.*, 6(3), 381–388 (1976). https://doi.org/10.1016/0008-8846(76)90101-0

Song, H.-W., Kwon, S.-J., Permeability characteristics of carbonated concrete considering capillary pore structure, *Cem. Concr. Res*., 37(6), 909–915 (2007). https://doi.org/10.1016/j.cemconres.2007.03.011

Song, H.-W., Kwon, S.-J., Byun, K.-J., Park, C.-K., Predicting carbonation in early-aged cracked concrete, *Cem. Concr. Res*., 36(5), 979–989 (2006). https://doi.org/10.1016/j.cemconres.2005.12.019

Song, K.-I., Song, J.-K., Lee, B. Y., Yang, K.-H., Carbonation Characteristics of Alkali-Activated Blast-Furnace Slag Mortar, *Adv. Mater. Sci. Eng*., 2014, 1–11(2014). https://doi.org/10.1155/2014/326458

Sulapha, P., Wong F., S., Wee T., H., Swaddiwudhipong, S., Carbonation of Concrete Containing Mineral Admixtures, *J. Mater. Civ. Eng.*, 15(2), 134–143(2003). https://doi.org/10.1061/(ASCE)0899-1561(2003)15:2(134)

Taffese, W. Z., Sistonen, E., Puttonen, J., CaPrM: Carbonation prediction model for reinforced concrete using machine learning methods, *Constr. Build. Mater.*, 100, 70–82(2015). https://doi.org/10.1016/j.conbuildmat.2015.09.058

Thiery, M., Villain, G., Dangla, P., Platret, G., Investigation of the carbonation front shape on cementitious materials: Effects of the chemical kinetics, *Cem. Concr. Res*., 37(7), 1047–1058(2007). https://doi.org/10.1016/j.cemconres.2007.04.002

Thomas, M. D. A., Matthews, J. D., Carbonation of fly ash concrete, *Mag. Concr. Res*., 44(160), 217–228(1992). https://doi.org/10.1680/macr.1992.44.160.217

Thomas, M. D. A., Osborne, G. J., Matthewst, J. D., Cripwell, J. B., A comparison of the properties of OPC, PFA and ggbs concretes in reinforced concrete tank walls of slender section, *Mag. Concr. Res.*, 42(152), 127–134(1990). https://doi.org/10.1680/macr.1990.42.152.127

Tuutti, K., Corrosion of steel in concrete, Corrosion of steel in concrete, Swedish Cement and Concrete Research Institute Stockholm, Stockholm, 1982.

Valcuende, M., Parra, C., Natural carbonation of self-compacting concretes, *Constr. Build. Mater*., 24(5), 848–853(2010). https://doi.org/10.1016/j.conbuildmat.2009.10.021

Verbeck, G. J., Mechanisms of Corrosion of Steel in Concrete, *Spec. Publ*., 49, 21–38(1975). https://doi.org/10.14359/17530

Wang, X.-Y., Lee, H.-S., A model for predicting the carbonation depth of concrete containing low-calcium fly ash, *Constr. Build. Mater*., 23(2), 725–733(2009). https://doi.org/10.1016/j.conbuildmat.2008.02.019

Wierig HJ, Longtime studies on the carbonation of concrete under normal outdoor exposure, In: RILE [M Symposium on Durability of Concrete under Normal Outdoor Exposure. Hannover, pp 239–249

Xue, B., Pei, J., Sheng, Y., Li, R., Effect of curing compounds on the properties and microstructure of cement concretes, *Constr. Build. Mater*., 101, 410–416(2015). https://doi.org/10.1016/j.conbuildmat.2015.10.124